

Nuclear magnetic resonance of ^{55}Mn in the antiferromagnet CsMnBr_3 in a variable longitudinal magnetic field

B. S. Dumesh*)

Institute of Spectroscopy, Russian Academy of Sciences, 142092 Troitsk, Moscow Region, Russia

M. I. Kurkin

Institute of Metal Physics, Urals Branch of the Russian Academy of Sciences, 620219 Ekaterinburg, Russia

S. V. Petrov and A. M. Tikhonov

P. L. Kapitza Institute of Physics Problems, Russian Academy of Sciences, 117334 Moscow, Russia
(Submitted 20 January 1999)

Zh. Éksp. Teor. Fiz. **115**, 2228–2241 (June 1999)

The spectrum and intensities of NMR lines are investigated experimentally and theoretically for excitation by an alternating magnetic field \mathbf{h}_{\parallel} parallel to a static field \mathbf{H} in the quasi-one-dimensional, six-sublattice antiferromagnet CsMnBr_3 . According to theory, two new NMR lines, which are not excited by a transverse magnetic field \mathbf{h}_{\perp} , are observed near the phase transition from triangular to collinear structure ($H = H_c$) [JETP **86**, 197 (1998)]. © 1999 American Institute of Physics. [S1063-7761(99)02506-8]

1. INTRODUCTION

The application of NMR methods to studies of the magnetic properties of quasi-one-dimensional, multiple-sublattice antiferromagnets has already helped to produce nontrivial results, such as the phenomenon of suppression of quantum fluctuations of electron spins¹ and a new type of magnetic structure in the easy-axis triangular antiferromagnet CsMnI_3 .² Nonetheless, it has become increasingly obvious that the full potential of NMR in such investigations have yet to be fully exploited. In this paper we discuss results obtained in the excitation of NMR by a longitudinal alternating magnetic field \mathbf{h}_{\parallel} parallel to a static magnetic field \mathbf{H} . This method has been successful in disclosing two additional NMR lines that are not excited by a transverse rf magnetic field \mathbf{h}_{\perp} . These lines are intriguing in that they exhibit a dynamic frequency shift near the phase transition from triangular to collinear structure.

In Secs. 2 and 3 of the present paper, we describe the magnetic properties of CsMnBr_3 and experiments on the observation of ^{55}Mn NMR for \mathbf{h}_{\parallel} . In Sec. 4 we give the results of calculations of the spectrum and intensities of NMR lines for various excitation techniques. In the Conclusion we discuss the suppression of steady-state NMR signals in the presence of large dynamic frequency shifts and the possibilities inherent in the parametric excitation of nuclear spins.

2. MAGNETIC PROPERTIES OF CsMnBr_3

The compound CsMnBr_3 is one of the family of halides of the type ABX_3 , where A denotes an alkali metal, B is a 3d metal, and X is a halogen. The crystal structure of CsMnBr_3 is described by the spatial symmetry group D_{6h}^4 , the Mn^{2+} ions forming a hexagonal grid in the basal plane (perpendicular to the C_6 axis).⁴ The crystal lattice determines the

detailed magnetic structure of this compound.^{5–9} The principal distinguishing feature of the lattice is that the distance between adjacent planes of magnetic ions is half the distance between nearest-neighbor ions within one plane. As a result, antiferromagnetic exchange interaction of the magnetic moments within chains running along the C_6 axis is 10^3 times the interchain antiferromagnetic exchange. This quasi-one-dimensionality significantly affects the magnetic properties, thus accounting for the heightened interest in the study of this class of materials.

The easy-axis character of the magnetic anisotropy in conjunction with antiferromagnetic interchain exchange results in the formation of a noncollinear, six-sublattice magnetic structure (Fig. 1a). Intrachain exchange induces antiferromagnetic ordering of the magnetic moments \mathbf{M}_j ($j = 1 - 6$) of three pairs of electronic sublattices, which is described by the antiferromagnetism vectors

$$\mathbf{L}_1 = \mathbf{M}_1 - \mathbf{M}_4, \quad \mathbf{L}_2 = \mathbf{M}_2 - \mathbf{M}_6, \quad \mathbf{L}_3 = \mathbf{M}_3 - \mathbf{M}_5.$$

Because of the vanishingly weak magnetic anisotropy in the basal plane, the sublattices in a weak magnetic field $\mathbf{H} \perp \text{C}_6$ are oriented in such a way that one of the indicated vectors \mathbf{L}_i , say \mathbf{L}_1 , is perpendicular to \mathbf{H} (Fig. 1a). The other two vectors, \mathbf{L}_2 , \mathbf{L}_3 , form angles close to 30° and 150° with \mathbf{H} .

As \mathbf{H} is increased, the angle α between \mathbf{L}_2 and \mathbf{L}_3 varies according to the law¹⁰

$$\cos \frac{\alpha}{2} = \frac{1}{2-z}, \quad z = \frac{H^2}{H_c^2}, \quad (1)$$

where $H_c = \sqrt{H_E H_{E'}} \approx 61$ kOe (at $T = 1.8$ K, Ref. 9), $H_E \approx 1500$ kOe, and $H_{E'} \approx 3$ kOe are the effective fields of intrachain and interchain exchange interactions, respectively.

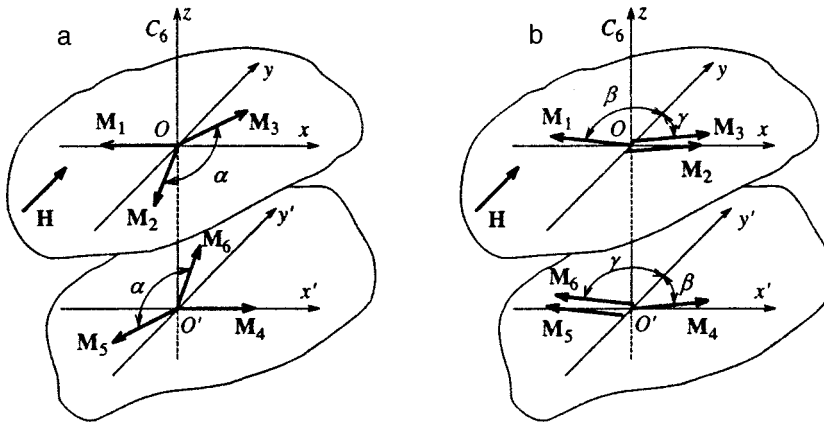


FIG. 1. Schematic representation of the magnetic structure of CsMnBr₃: a) $H \ll H_c$; b) $H > H_c$ ($\beta = \gamma$).

In a field $H = H_c$ the above-described magnetic structure changes to a collinear configuration ($\alpha = 0$), corresponding to a second-order phase transition (Fig. 1b).

The magnetic field of the nuclei of the j th sublattice is determined by the sum of the external field \mathbf{H} and the hyperfine fields \mathbf{H}_{nj} :

$$H_j = |\mathbf{H}_{nj} + \mathbf{H}| = H_n \sqrt{1 + \frac{H^2}{H_n^2} - 2 \frac{H}{H_n} \cos \theta_j}, \quad (2)$$

where $H_n = -AM_0$, M_0 is the average magnetic moment of the sublattice, A is the hyperfine interaction constant, and θ_j is the angle between \mathbf{H} and \mathbf{M}_j :

$$\begin{aligned} \cos \theta_{1,4} &= \frac{H}{H_E}, \\ \cos \theta_{2,5} &= -\sin \frac{\alpha}{2} + \frac{H}{H_E} \cos^2 \frac{\alpha}{2} + o\left(\frac{H}{H_E}\right), \\ \cos \theta_{3,6} &= \sin \frac{\alpha}{2} + \frac{H}{H_E} \cos^2 \frac{\alpha}{2} + o\left(\frac{H}{H_E}\right). \end{aligned} \quad (3)$$

Consequently, for $H < H_c$ there must be three twofold degenerate NMR branches $\omega_{nj} = \gamma_n H_j$.

In weak fields H the degeneracy is lifted by interaction with the Goldstone antiferromagnetic resonance (AFMR) mode. The frequencies of the three NMR branches (Ω_4 , Ω_5 , and Ω_6) decrease (this is the so-called dynamic frequency shift). Their spectrum has been investigated experimentally and theoretically.^{1,3} A functional dependence $H_n(H)$ that differs for spins in sublattices 1, 4 and 2, 3, 5, 6 has also been reported in the cited papers, owing to the suppression of quantum fluctuations of the magnetic field and a corresponding increase in $M_j(H)$. The spectrum of all other branches is described by Eqs. (2) and (3) with the functional $H_{nj}(H)$ taken into account, but NMR signal amplification does not take place for these branches, and they have not been observed experimentally.

As $H \rightarrow H_c$, two of these branches begin to interact with the AFMR mode ω_5 (in the notation of Ref. 8), whose frequency tends to zero as phase transition is approached. The spectrum of these branches is deformed in this case, and the

branches themselves become observable in excitation by an rf field \mathbf{h}_{\parallel} . These phenomena are the subject of the present article.

3. MEASUREMENT PROCEDURE AND DESCRIPTION OF THE EXPERIMENT

The objects of investigation were CsMnBr₃ single crystals grown and oriented as in Ref. 3, which also describes the wide-range continuous NMR spectrometer used to perform the measurements. The main difference is a modification of the cavity structure to impart the required polarization to the rf field \mathbf{h}_{\parallel} . A block diagram of the resonance circuit is shown in Fig. 2. A movable copper plate 2 with a dielectric coating 3 forms with the casing an additional variable capacitance, which is used to tune the cavity frequency. A narrow slot 7 forms the structural capacitance of the loop. The two-headed arrow indicates the directions of motion of the plate. The whole structure is positioned in a superconducting

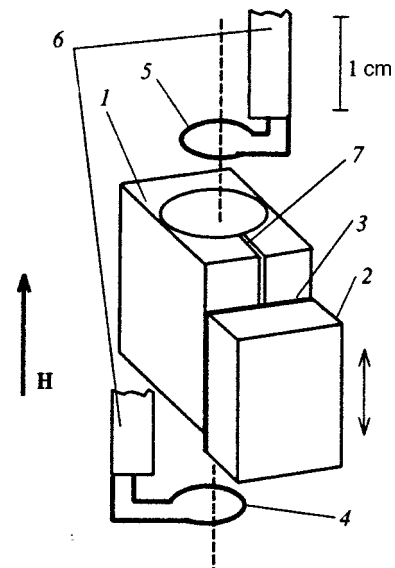


FIG. 2. Block diagram of the resonance circuit: (1) cavity; (2) movable copper plate; (3) thin insulating film; (4, 5) coupling loops; (6) coaxial leads; (7) narrow slot.

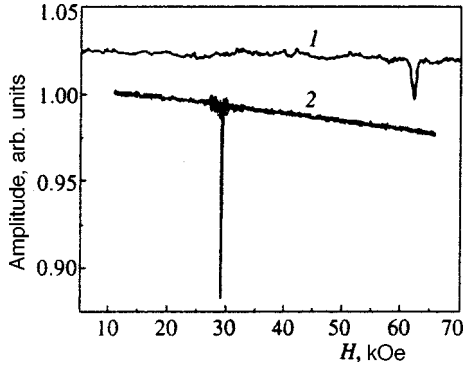


FIG. 3. Experimental absorption signal in CsMnBr₃ ($\mathbf{H} \perp C_6$) at $T=1.3$ K and 349.6 MHz with excitation by alternating magnetic fields \mathbf{h}_{\parallel} (curve 1) and \mathbf{h}_{\perp} (curve 2).

solenoid with an inside diameter of 25 mm, and the rf field is precisely parallel to the field of the solenoid \mathbf{H} .

We used two cavities with $Q \approx 400$ at 4.2 K. The frequency tuning range of one cavity was from 390 MHz to 470 MHz, and the range of the other was from 310 MHz to 380 MHz. The cavity containing the investigated single-crystal sample was placed directly in a helium tank. An external magnetic field was applied perpendicular to the hexagonal C_6 axis of the crystal. In all other respects the spectrometer and the measurement procedure were identical to those in Ref. 3.

Figure 3 shows the absorption signal in CsMnBr₃ for $T=1.3$ K, a frequency of 349.6 MHz, and fields \mathbf{h}_{\parallel} (curve 1) and \mathbf{h}_{\perp} (curve 2). It is evident that different NMR branches are excited in these two cases. The NMR spectrum in CsMnBr₃ for $\mathbf{h}_{\parallel} \perp C_6$ at $T=1.3$ K is represented by light circles in Fig. 4. NMR is observed close to H_c over a broad frequency range, demonstrating the large dynamic frequency shift of NMR. As $|H-H_c|$ increases, the intensity of the signal decreases, and its position approaches the unshifted NMR spectrum, which is represented by dashed curves. The solid curves represent the NMR spectrum calculated from Eqs. (20) and (21) below. We have not used any fitting constants here. Satisfactory agreement is observed between the

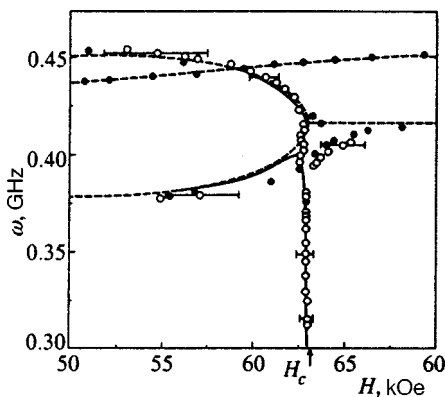


FIG. 4. NMR spectrum in CsMnBr₃ for $\mathbf{H} \perp C_6$ at $T=1.3$ K with excitation by alternating magnetic fields \mathbf{h}_{\parallel} (light circles) and \mathbf{h}_{\perp} (heavy dots, from Ref. 3).

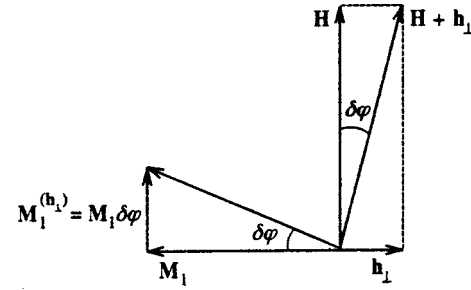


FIG. 5. Influence of \mathbf{h}_{\perp} on the orientation of \mathbf{M} .

experimental and calculated spectra. The observed differences are attributable to the appreciable width of the AFMR line near phase transition.

It must be noted that NMR in parallel fields has heretofore been observed only in superfluid helium ³He and in the domain walls of ferromagnets. In our case NMR is generated in a homogeneous sample, because the signal is observed at a large distance from the phase transition field.

Consequently, five NMR modes are observed in CsMnBr₃. Three of them are excited for \mathbf{h}_{\perp} , interact with the Goldstone AFMR mode, and are observed in the range of fields 20–80 kOe.³ Two modes are generated for \mathbf{h}_{\parallel} , interact with the AFMR mode ω_5 , and are observed in fields of 50–65 kOe.

4. THEORY

We analyze the intensities of NMR lines excited by various techniques, using the same equations for the magnetizations \mathbf{m}_j ($j=1, \dots, 6$) of the nuclear sublattices as in Ref. 3. Now, however, in these equations we need to take into account, first, interaction with differently polarized alternating fields \mathbf{h} and, second, nuclear magnetic relaxation, which takes the oscillations of \mathbf{m}_j into the steady state. We treat relaxation processes in the relaxation time approximation, which corresponds to the Bloch equations¹¹ (see Appendix).

Figure 5 shows the influence of a transverse field \mathbf{h}_{\perp} on the orientation of the vector \mathbf{M}_1 when the frequency of the alternating field is much lower than the AFMR frequency (at NMR frequencies this condition is easily satisfied at any H , owing to the hyperfine gap in the AFMR spectrum^{12,13}). It is evident that for $h_{\perp} \ll H$ everything reduces to rotation through the angle $\delta\varphi = h_{\perp}/H$. All other vectors \mathbf{M}_j rotate through the same angle, and their variations are therefore described by the equations

$$\mathbf{M}_j^{(h_{\perp})}(t) = \mathbf{M}_j \delta\varphi = \chi_{\perp} \mathbf{h}_{\perp}(t), \quad (4)$$

where

$$\chi_{\perp} = M_j/H \quad (5)$$

is the magnetic susceptibility in a field h_{\perp} . It follows from Fig. 1 that a longitudinal field \mathbf{h}_{\parallel} has scarcely any influence on the orientation of the vectors \mathbf{M}_1 and \mathbf{M}_4 , but changes the angle α by

$$\delta\alpha = \begin{cases} 4Hh_{\parallel} / \sqrt{(3H_c^2 - H^2)(H_c^2 - H^2)}, & H \leq H_c, \\ 0, & H > H_c. \end{cases} \quad (6)$$

Equations (6) can be derived from Eq. (1) by writing the latter for the field $H + h_{\parallel}$ and expanding in powers of h_{\parallel} . The calculation of the variations of the vectors \mathbf{M}_j for such a variation of the angle α leads to the equations

$$\mathbf{M}_j^{(h_{\parallel})}(t) = \chi_{\parallel j} \mathbf{h}_{\parallel}(t), \quad (7)$$

where

$$\chi_{\parallel 1} = \chi_{\parallel 4} = 0, \quad \chi_{\parallel 2} = \chi_{\parallel 6} = -\chi_{\parallel 3} = -\chi_{\parallel 5} = \chi_{\parallel}, \quad (8)$$

$$\chi_{\parallel}(H) = \begin{cases} M_0 \delta\alpha / 2h_{\parallel}, & H \leq H_c, \\ 0, & H > H_c. \end{cases} \quad (9)$$

We have thus calculated the NMR gains:

$$\begin{aligned} \eta_{\perp} &= A\chi_{\perp} = H_n/H, \\ \eta_{\parallel j} &= A\chi_{\parallel j}. \end{aligned} \quad (10)$$

In the Appendix we show that the use of Eqs. (6)–(9) in the equations for \mathbf{m}_j permits them to be written in the form (A12):

$$\begin{aligned} &\left[\left(\omega + \frac{i}{T_2} \right)^2 - \omega_{nj}^2 \right] m_{x_j}(\omega) \\ &+ \gamma_n \omega_{nj} A m_{z_j} \frac{H_n}{H_c} \sum_j \lambda_{jj'} m_{x_{j'}}(\omega) \\ &+ \gamma_n \omega_{nj} m_{z_j} \eta_{\perp} h_{\perp}(\omega) + \gamma_n \omega_{nj} m_{z_j} \eta_{\parallel j} h_{\parallel}(\omega) = 0. \end{aligned} \quad (11)$$

The Appendix also gives expressions for the quantities $\lambda_{jj'}$ (A7) and ω_{nj} (A13). The expressions for $m_{x_j}(\omega)$, $h_{\perp}(\omega)$, and $h_{\parallel}(\omega)$ are related to $m_{x_j}(t)$, $h_{\perp}(t)$, and $h_{\parallel}(t)$ by the Fourier transform (48).

The determinant of the system of equations (11) characterizes the six NMR frequencies. We note that the frequencies of only three of these lines, excited by a transverse field \mathbf{h}_{\perp} , were analyzed in Ref. 3. We now look into the feasibility of exciting all six lines.

Taking the amplification into account, we describe the intensity $I_n(\omega)$ of the absorption signal measured in the experiments of Ref. 3 by the equation

$$I_n(\omega) = \sum_j \eta_j \text{Im} m_{x_j}(\omega), \quad (12)$$

where $\text{Im} m_{x_j}(\omega)$ is the imaginary part of the solution of the system (11) for the frequency ω . These equations have the simplest form in the cases $H \ll H_c$, $H \approx H_c$, and $H > H_c$. An analysis of the cases $H \ll H_c$ and $H > H_c$ yields results that agree with the curves in Refs. 1 and 3 to within the experimental errors. We therefore confine our discussion to the case $H \approx H_c$ only, as it is associated with new experimental results described in the preceding section of the article.

For $H \approx H_c$ the following expressions for $\lambda_{jj'}$ can be obtained from Eq. (A7):

$$\begin{aligned} \lambda_{22} = \lambda_{33} = \lambda_{55} = \lambda_{66} = \lambda_{26} = \lambda_{35} = -\lambda_{23} = -\lambda_{63} = -\lambda_{25} \\ = -\lambda_{56} = 0.5 \{ 2[1 - (H/H_c)^2] + \epsilon \}^{-1}, \end{aligned} \quad (13)$$

where $\epsilon = 2m_0/H_{E'} \approx 10^{-2}$ [see Eq. (A5)].

The components λ_{1j} and λ_{4j} do not have singularities at $H = H_c$, and their influence can therefore be disregarded. A second procedure by which it is possible to substantially simplify the system of equations (11) involves the transformation to new variables $m_{k\pm}$ ($k = 1, 2, 3$):

$$m_{1\pm} = m_{x_1} \pm m_{x_4}, \quad m_{2\pm} = m_{x_2} \pm m_{x_5}, \quad m_{3\pm} = m_{x_3} \pm m_{x_6}. \quad (14)$$

As a result, the system (11) is decomposed into four independent equations:

$$\begin{aligned} &\left[\left(\omega + \frac{i}{T_2} \right)^2 - \omega_{n1}^2 \right] m_{1-} = 0, \\ &\left[\left(\omega + \frac{i}{T_2} \right)^2 - \omega_{nk}^2 \right] m_{k+} + 2\omega_{nk} m_0 \gamma_n \eta_{\perp} h_{\perp} = 0, \quad k = 1, 2, 3, \end{aligned} \quad (15)$$

and a system of two coupled equations:

$$\begin{aligned} &\left[\left(\omega + \frac{i}{T_2} \right)^2 - \omega_{n2}^2 \right] m_{2-} + \frac{1}{2} \omega_{n2} \omega_{pc}(H) \frac{m_z}{m_0} (m_{2-} \\ &\quad - m_{3-}) + 2\omega_{n2} \gamma_n \eta_{\parallel} h_{\parallel} m_z = 0, \\ &\left[\left(\omega + \frac{i}{T_2} \right)^2 - \omega_{n3}^2 \right] m_{3-} + \frac{1}{2} \omega_{n3} \omega_{pc}(H) \frac{m_z}{m_0} (m_{3-} \\ &\quad - m_{2-}) + 2\omega_{n3} \gamma_n \eta_{\parallel} h_{\parallel} m_z = 0, \end{aligned} \quad (16)$$

where the two quantities

$$\omega_{pc}(H) = \frac{\omega_{n2}(H_c) \epsilon}{[\epsilon + 2(1 - (H/H_c)^2)]} \quad (17)$$

and

$$\eta_{\parallel} = H_n / \sqrt{H_c(H_c - H)}, \quad (18)$$

have singularities at $H = H_c$. According to Eqs. (15), the component in the NMR spectrum corresponding to m_{1-} is not excited by the variable field, and the m_{k+} components are excited by the transverse field \mathbf{h}_{\perp} . The spectrum of these components is represented by dots in Fig. 4, and their properties are discussed in Ref. 3. The new results, represented by the open circles in Fig. 4, are described by the solutions of Eqs. (16). Their form depends strongly on the ratio between the difference in the frequencies ω_{n2} and ω_{n3} (45),

$$\Delta = \omega_{n2} - \omega_{n3} = 2H \sin(\alpha/2), \quad (19)$$

and the quantity ω_{pc} (17). For $\Delta \gg \omega_{pc}$ the frequencies of the components m_{2-} and m_{3-} differ from the frequencies of the components m_{2+} and m_{3+} excited by the field \mathbf{h}_{\perp} , consistent with the results shown in Fig. 4. For $\Delta \ll \omega_{pc}$ the following equations can be obtained for the frequencies of the components m_{2-} and m_{3-} , which are the roots of the secular equation for (16):

$$\Omega_2^2 = 0.5[\omega_{n2}^2(H) + \omega_{n3}^2(H)], \quad \Omega_3^2 = \Omega_2[\Omega_2 - \omega_{pc}(H)]. \quad (20)$$

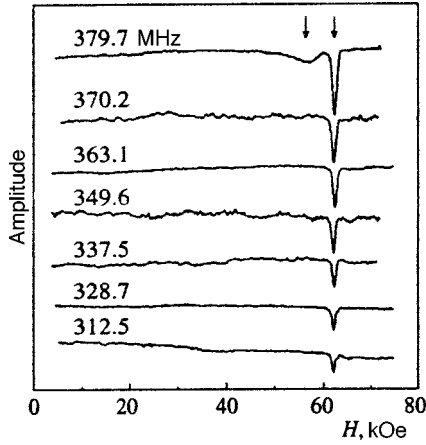


FIG. 6. Experimental traces of the low-frequency NMR branch $\Omega_3(H)$ at $T=1.3$ K and several frequencies. The arrows indicate the midpoints of the NMR lines at 379.7 MHz.

As $H \rightarrow H_c$, the frequency Ω_2 approaches $\omega_{n2}(H_c) = \gamma_n A M_0$ (45), and Ω_3 (taking (17) into account) tends to zero:

$$\Omega_3^2(H) = \Omega_2^2(H_c) \frac{1 - (H/H_c)^2}{\epsilon/2 + 1 - (H/H_c)^2}. \quad (21)$$

The spectra calculated from these equations are represented by solid curves in Fig. 4.

Equations for the intensities $I_n(\omega)$ of the NMR lines at the frequencies Ω_2 and Ω_3 can be obtained by substituting the corresponding solutions of the system (16) into Eq. (12):

$$I_n(\Omega_3) = 2m_0 \eta_{\parallel}^2 \gamma_n h_{\parallel} T_2, \quad (22)$$

$$I_n(\Omega_2) = 4I_n(\Omega_3) \left[\frac{\gamma_n H}{\omega_{pc}(H)} \right]^2 \sin^2 \frac{\alpha}{2}. \quad (23)$$

It follows from Eqs. (18), (21), and (22) that the intensity

$$I_n(\Omega_3) \propto \eta_{\parallel}^2 \propto \frac{1}{H_c - H} \propto \frac{1}{\Omega_3(H)} \quad (24)$$

should increase as $\Omega_3(H)$ decreases. It is evident from Fig. 6 that it decreases in the experiment. The reason for this disparity is that Eqs. (22) and (23) have been obtained from the solution of the system (16) in the approximation $m_z = m_0$. If this is not done, Eq. (20) has the form

$$\Omega_3^2 = \Omega_2 [\Omega_2 - \omega_{pc}(H) m_z / m_0]. \quad (25)$$

Inasmuch as $m_0^2 = m_x^2 + m_y^2 + m_z^2$, the dependence of Ω_3 on m_z implies a dependence of Ω_3 on the amplitude of the oscillations of the magnetizations of the nuclear sublattices m_j . In other words, whereas the oscillations of m_j are in resonance with the alternating field at small amplitudes, the resonance conditions begin to break down as this amplitude increases, doing so more rapidly the higher the frequency $\omega_{pc}(H)$ and, accordingly, the lower the frequency Ω_3 . Hence it follows that for sufficiently high $\omega_{pc}(H)$ the intensity $I_n(\Omega_3)$ begins to decrease as Ω_3 decreases.

The influence of various nonlinear effects on the steady-state NMR signals in the presence of a dynamic frequency

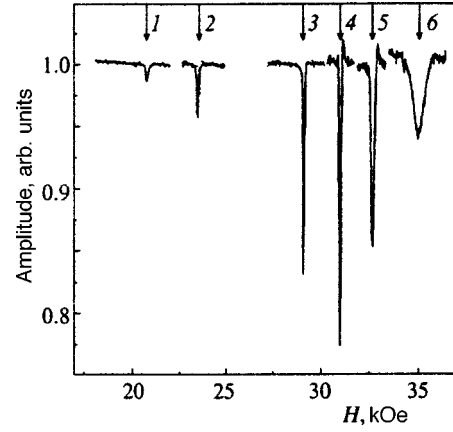


FIG. 7. Experimental low-frequency NMR branch $\Omega_4(H)$ at $T=1.3$ K and various frequencies: (1) 220.1 MHz; (2) 273.7 MHz; (3) 350.1 MHz; (4) 363.0 MHz; (5) 370.0 MHz; (6) 375.2 MHz.

shift has been analyzed previously.^{11,13–18} If the equations given in the cited papers are used, the following relation between $I_n(\Omega_3)$ and Ω_3 can be obtained in the investigated frequency range of 310–380 MHz:

$$I_n(\Omega_3) \propto \Omega_3^{1/3}, \quad (26)$$

which agrees qualitatively with the results in Fig. 6. To make a quantitative comparison, the influence of inhomogeneities of the sample must also be taken into account in the theory, because we are now in the vicinity of the phase transition.

5. CONCLUSION

It follows from Fig. 6 that the decrease in the intensity of the steady-state NMR signals due to nonlinear effects strongly limits the frequency range in which such signals can be observed near H_c . A similar difficulty is encountered in weak fields $H \ll H_c$.^{1,3} In this case the dynamic frequency shift is observed over a far broader range of fields H than merely in the vicinity of H_c , so that the NMR signals shown in Fig. 7 exhibit not only the values of the frequencies Ω , but also the fields H . It is evident from Fig. 7 that as H and Ω decrease (i.e., as the dynamic frequency shift increases), the signal intensity first increases and then decreases. If Eqs. (11), with nonlinear effects taken into account, are used to describe these signals, the following relation can be obtained for their intensities $I_n(\Omega)$ (12):

$$I_n(\Omega) \propto \eta_{\perp}^2 \propto H^{-2}, \quad (27)$$

where η_{\perp}^2 is given by Eq. (10). Like Eq. (24), this relation describes the increase in $I_n(\Omega)$ as Ω decreases. For larger dynamic frequency shifts, such that nonlinear effects become appreciable, it is necessary to use the same expressions for I_n as those from which the relation (26) is obtained. Then in place of (27) we can obtain a dependence of the form

$$I_n(\Omega_4) \propto H^{10/3}, \quad (28)$$

which dictates that I_n decreases as H decreases.

There are three ways to approach the investigation of the nuclear spin properties at lower frequencies (for larger dynamic frequency shifts). First, the amplitude of the exciting

field can be raised to levels such that hysteresis effects begin to set in as a result of the nonlinearity of the dynamic frequency shift.^{13–16} Tulin¹⁷ investigated these effects experimentally for three-dimensional antiferromagnets (MnCO_3 and CsMnF_3), but he worked with weak fields H of the order of 1 kOe or less, for which the gain η_{\perp} (10) is large. At $H \approx 20$ kOe, η_{\perp} is much smaller, so that the investigation of hysteresis effects in the case of CsMnBr_3 requires more powerful rf field generators.

Second, NMR pulse techniques can be used, and echo signals in particular. Owing to the mechanism by which such signals are generated as a result of modulation of the NMR frequency, a certain reserve is available for increasing their amplitude in the presence of a large dynamic frequency shift. The feasibility of using NMR pulse signals to study the properties of nuclear spins with a large dynamic frequency shift has been discussed in detail.¹⁸

The third possibility for the investigation of NMR signals in the presence of a large dynamic frequency shift involves the parametric excitation of nuclear spins by parallel pumping.¹⁹ This method is based on the fact that under the conditions of a dynamic frequency shift, the precession of the nuclear magnetic moments normally becomes elliptical, with an eccentricity that depends on the magnetic field. As a result, an alternating magnetic field \mathbf{h}_{\parallel} at twice the NMR frequency imparts parametric instability to such precession if the amplitude $h(t)$ exceeds the threshold level h_0 . Equations (11) then lead to an expression for h_0 ,

$$h_0(\omega) = \frac{2}{T_2 |\partial \omega_p / \partial H|}, \quad (29)$$

where ω_p is the dynamic frequency shift parameter. In CsMnBr_3 a large dynamic frequency shift occurs in two cases: a) for $H \approx H_c$, when $\omega_p(H_c) = \omega_{pc}$ (17); b) for $H \ll H_c$, when $\omega_p(H)$ is given by

$$\omega_p = \frac{12\epsilon\omega_{n1}}{9(H/H_c)^6 + 12\epsilon}. \quad (30)$$

Equation (29) is transformed as follows for these two cases:

a) for $H \approx H_c$ and $\epsilon \ll |1 - (H/H_c)^2|$

$$h_0 = \frac{H_c |1 - (H/H_c)^2|}{\omega_{pc}(H_c) T_2}; \quad (31)$$

b) for $H \ll H_c$ and $\epsilon \ll H/H_c$

$$h_0 = \frac{H}{3\omega_p(H) T_2}. \quad (32)$$

Equations (31) and (32) can also be used to analyze the threshold amplitude in the parametric pumping of nuclear spin waves.^{20–22} It is sufficient here to replace T_2 and ω_p by $T_2(q)$ and $\omega_p(q)$, where q is the wave vector.

It is clear from these equations that the threshold amplitude h_0 drops as ω_p increases. This means that when the dynamic frequency shift increases, the conditions for the observation of parametric NMR improve, rather than deteriorating as in the case of steady-state NMR.

In closing, the authors wish to extend their sincere thanks to N. M. Kreĭnes, L. A. Prozorov, A. I. Smirnov, and

I. A. Fomin for a productive discussion and critical remarks. This work received financial support from the Russian Fund for Fundamental Research (Projects 96-02-16489 and 98-02-16572).

APPENDIX

As mentioned in the Introduction, the equations used in Ref. 3 to analyze the spectrum of NMR frequencies can be applied to the calculation of the intensities of steady-state NMR signals. To do so, however, the equations must be modified to account for interactions with the external alternating magnetic field and with the fluctuating fields responsible for nuclear magnetic relaxation. If direct interaction of the magnetizations \mathbf{m}_j of the nuclear sublattices with the alternating field is ignored (by virtue of amplitude effects¹¹) and if interaction with the fluctuating fields is taken into account in the relaxation time approximation, it is possible to obtain a system of equations that coincides with the usual Bloch equations²³ in the external magnetic field \mathbf{H} and the hyperfine field $\mathbf{H}_{nj} = A\mathbf{M}_j$ (Ref. 11):

$$\begin{aligned} \frac{dm_{x_j}}{dt} &= \gamma_n (AM_{z_j} + H_{z_j}) m_{y_j} - \frac{m_{x_j}}{T_2}, \\ \frac{dm_{y_j}}{dt} &= -\gamma_n (AM_{z_j} + H_{z_j}) m_{x_j} + \gamma_n m_{z_j} AM_{x_j} - \frac{m_{y_j}}{T_2}, \end{aligned} \quad (A1)$$

where (x_j, y_j, z_j) denotes the coordinate systems associated with equilibrium orientations of the vectors $\mathbf{m}_j \parallel \mathbf{H}_{nj} \parallel \mathbf{M}_j$ (we disregard the deviation of the orientation of the field $\mathbf{H}_{nj} + \mathbf{H}$ from the hyperfine field \mathbf{H}_{nj} , since $H_{nj} \gg H$), A is the hyperfine interaction constant, γ_n is the nuclear gyromagnetic ratio, and T_2 is the transverse nuclear magnetic relaxation time.

For small oscillations of m_j the components m_{z_j} can almost always be replaced by the equilibrium value m_0 . An exception is encountered for oscillations with a large dynamic frequency shift, when nonlinear effects become significant, and the variation of the components m_{z_j} must be taken into account. In CsMnBr_3 , however, as opposed to two-sublattice, three-dimensional antiferromagnets, these effects do not exhibit any specific attributes, so that the equations derived in Refs. 13–18 can be used.

In the description of NMR experiments the magnetization components M_{z_j} of the electronic sublattices can always be replaced by the equilibrium values M_j (by virtue of the weak influence of hyperfine interaction on the oscillations of M_j).

The components M_{y_j} do not occur in Eqs. (A1). As in Ref. 3, they are disregarded, because strong uniaxial anisotropy prevents the sublattices from leaving the basal plane ($M_{y_j} \ll M_{x_j}$). The components M_{x_j} in Eq. (A1) can be written as a three-term sum

$$M_{x_j} = M_{x_j}^{(h_{\perp})} + M_{x_j}^{(h_{\parallel})} + M_{x_j}^{(m)}, \quad (A2)$$

where $M^{(h_{\perp})}$ and $M^{(h_{\parallel})}$ are attributable to interaction with the transverse (\mathbf{h}_{\perp}) and longitudinal (\mathbf{h}_{\parallel}) alternating magnetic fields, and the components $M_{x_j}^{(m)}$ are attributable to hyperfine

interaction with the oscillations of \mathbf{m}_j . The equations used to calculate $M_{x_j}^{(m)}$ in Ref. 3 take into account only one low-frequency AFMR branch. Here we have made use of the fact that the NMR frequencies are very much lower than the AFMR frequencies (with allowance for the hyperfine gap in the spectrum of magnons¹²), so that the kinetic energy can be neglected in the expression for the Lagrangian describing the behavior of \mathbf{M}_j (Ref. 24). In this approximation, equations for M_{x_j} can be obtained by minimizing the potential energy with hyperfine interaction taken into account. We can now obtain equations that are valid for any fields H , despite the difference in the symmetries of the soft modes for $H=0$ and $H=H_c$:

$$\begin{aligned} a_1 M_{x_1}^{(m)} - b_1 (M_{x_2}^{(m)} + M_{x_3}^{(m)}) &= (H_n/H_{E'}) (m_{x_1} + m_{x_4}), \\ -b_1 M_{x_1}^{(m)} + a_2 M_{x_2}^{(m)} + b_2 M_{x_3}^{(m)} &= (H_n/H_{E'}) (m_{x_2} + m_{x_6}), \\ -b_1 M_{x_1}^{(m)} + b_2 M_{x_2}^{(m)} + a_2 M_{x_3}^{(m)} &= (H_n/H_{E'}) (m_{x_3} + m_{x_6}), \end{aligned} \quad (\text{A3})$$

$$M_{x_1}^{(m)} = M_{x_4}^{(m)}, \quad M_{x_2}^{(m)} = M_{x_6}^{(m)}, \quad M_{x_3}^{(m)} = M_{x_5}^{(m)}, \quad (\text{A4})$$

where $H_n = AM_0$,

$$\begin{aligned} b_1 &= \cos \frac{\alpha}{2} = \frac{1}{2 - (H/H_c)^2}, \quad b_2 = \cos \alpha = 2b_1^2 - 1, \\ a_1 &= \left(\frac{H}{H_c}\right)^2 + 2b_1 + \epsilon, \quad a_2 = b_1 - \left[1 - \left(\frac{H}{H_c}\right)^2\right] b_2 + \epsilon, \\ \epsilon &= \frac{2Am_0}{H_{E'}}, \end{aligned} \quad (\text{A5})$$

Am_0 is the static hyperfine field, which is conveyed by the nuclei to the electrons and is responsible for the hyperfine gap in the AFMR spectrum,¹¹ $H_{E'} = 3$ kOe is the effective in-plane exchange field, α is the angle between the vectors \mathbf{M}_2 and \mathbf{M}_3 (Fig. 1), and H_c is the critical field for transition to the collinear phase. At $T > 1$ K we have

$$\epsilon = \frac{2Am_0}{H_{E'}} = \frac{2H_n}{H_{E'}} \frac{\gamma_n \hbar \gamma_n H_n}{\gamma_e kT} \ll 10^{-2},$$

so that only linear corrections in ϵ will be taken into account below. The solution of the system (A3), (A4) has the form

$$M_{x_j}^{(m)} = \frac{H_n}{H_{E'}} \sum_{j'} \lambda_{jj'} m_{x_{j'}}, \quad (\text{A6})$$

where

$$\begin{aligned} \lambda_{11} &= \lambda_{44} = (a_2^2 - b_2^2)/\mathcal{D}, \quad \lambda_{1j} = \lambda_{4j} = b_1(a_2 - b_2)/\mathcal{D}, \\ \lambda_{22} &= \lambda_{33} = \lambda_{55} = \lambda_{66} = \lambda_{26} = \lambda_{35} = (a_1 a_2 - b_1^2)/\mathcal{D}, \\ \lambda_{23} &= \lambda_{63} = \lambda_{25} = \lambda_{65} = (b_1^2 - a_1 b_2)/\mathcal{D}, \quad \lambda_{jj'} = \lambda_{j'j}; \end{aligned} \quad (\text{A7})$$

and

$$\mathcal{D} = (a_2 - b_2)[a_1(a_2 + b_2) - 2b_1^2] \quad (\text{A8})$$

is the determinant of the system (A3). For $H \leq H_c$, on the basis of (A5) and (A8), we have

$$\begin{aligned} \mathcal{D}(H) &= [b_1(H) + 1][1 - (H/H_c)^2 + \epsilon][3b_1(H)\epsilon \\ &\quad + (H/H_c)^6 b_1(H)(b_1(H) + 1)^2], \end{aligned} \quad (\text{A9})$$

and for $H \geq H_c$

$$\mathcal{D} = [(H/H_c)^2 - 1 + \epsilon](H/H_c)^2[(H/H_c)^2 + 3]. \quad (\text{A10})$$

At the points $H=0$ and $H=H_c$ the determinant $\mathcal{D}(H)$ attains the minimum values

$$\mathcal{D}(0) = 9\epsilon/4, \quad \mathcal{D}(H_c) = 4\epsilon, \quad (\text{A11})$$

and the components $M_{x_j}^{(m)}$ attain maxima.

Taking Eqs. (A2), (A6), (7), (9), and (10) into account, we can write Eq. (A1) in the form

$$\begin{aligned} \left[\left(\omega + \frac{i}{T_2} \right)^2 - \omega_{nj}^2 \right] m_{x_j}(\omega) \\ + \gamma_n \omega_{nj} A m_{z_j} \frac{H_n}{H_{E'}} \sum_{j'} \lambda_{jj'} m_{x_{j'}}(\omega) \\ + \gamma_n \omega_{nj} m_{z_j} \eta_{\perp} h_{\perp}(\omega) + \gamma_n \omega_{nj} m_{z_j} \eta_{\parallel} h_{\parallel}(\omega) = 0, \end{aligned} \quad (\text{A12})$$

where

$$\begin{aligned} \omega_{n1} &= \omega_{n4} = \gamma_n A M_1, \\ \omega_{n2} &= \omega_{n5} = \gamma_n A M_2 + H \sin(\alpha/2), \\ \omega_{n3} &= \omega_{n6} = \gamma_n A M_2 - H \sin(\alpha/2), \end{aligned} \quad (\text{A13})$$

are the unshifted (not perturbed by dynamic frequency shift) NMR frequencies, while

$$\eta_{\perp} = A \chi_{\perp} = H_n/H \quad (\text{A14})$$

and

$$\eta_{\parallel 2} = \eta_{\parallel 6} = -\eta_{\parallel 3} = -\eta_{\parallel 5} = \eta_{\parallel} = A \chi_{\parallel}, \quad \eta_{\parallel 1} = \eta_{\parallel 4} = 0 \quad (\text{A15})$$

are the gains for the field h_{\perp} and h_{\parallel} ; the variables $m_{x_j}(\omega)$, $h_{\perp}(\omega)$, and $h_{\parallel}(\omega)$ are related to $m_{x_j}(t)$, $h_{\perp}(t)$, and $h_{\parallel}(t)$ by the Fourier transform

$$m_{x_j}(\omega) = \int_{-\infty}^{+\infty} \exp(i\omega t) m_{x_j}(t) dt. \quad (\text{A16})$$

Analogous relations hold for $h_{\perp}(\omega)$ and $h_{\parallel}(\omega)$.

*¹E-mail: dumesh@isan.troitsk.ru

¹A. S. Borovik-Romanov, S. V. Petrov, A. M. Tikhonov, and B. S. Dumesh, JETP Lett. **66**, 759 (1997).

²B. S. Dumesh, S. V. Petrov, and A. M. Tikhonov, JETP Lett. **67**, 1046 (1998).

³A. S. Borovik-Romanov, B. S. Dumesh, S. V. Petrov, and A. M. Tikhonov, Zh. Eksp. Teor. Fiz. **113**, 352 (1998) [JETP **86**, 197 (1998)].

⁴J. Goodyear and D. J. Kennedy, Acta Crystallogr. Sect. B **28**, 1640 (1974).

⁵M. Eibischutz, R. C. Sherwood, F. S. L. Hsu, and D. E. Cox, in *Proceedings of the 18th Annual Conference on Magnetism and Magnetic Materials*, AIP Conf. Proc., No. 10, American Institute of Physics, New York (1973), p. 684.

- ⁶B. D. Gaulin, T. E. Mason, M. F. Collins, and J. Z. Larese, *Phys. Rev. Lett.* **62**, 1380 (1989).
- ⁷B. D. Gaulin, M. F. Collins, and W. J. L. Buyers, *J. Appl. Phys.* **61**, 3409 (1987).
- ⁸I. A. Zaliznyak, L. A. Prozorova, and S. V. Petrov, *Zh. Éksp. Teor. Fiz.* **97**, 359 (1989) [*Sov. Phys. JETP* **70**, 203 (1989)].
- ⁹S. I. Abarzhi, A. N. Bazhan, L. A. Prozorova, and I. A. Zaliznyak, *J. Phys.: Condens. Matter* **4**, 3307 (1992).
- ¹⁰A. V. Chubukov, *J. Phys. C Solid State Phys.* **21**, 441 (1988).
- ¹¹M. I. Kurkin and E. A. Turov, *Nuclear Magnetic Resonance in Magnetically Ordered Materials and Its Applications* [in Russian], Nauka, Moscow (1990).
- ¹²I. A. Zaliznyak, N. N. Zorin, and S. V. Petrov, *JETP Lett.* **64**, 473 (1996).
- ¹³P. G. De Gennes, P. Pincus, F. Hartmann-Bourtron, and J. M. Winter, *Phys. Rev.* **129**, 1105 (1963).
- ¹⁴M. I. Kurkin, *JETP Lett.* **28**, 628 (1978).
- ¹⁵M. I. Kurkin, Yu. G. Raïdugin, V. N. Sedyskhin, and F. P. Tankeev, *Fiz. Tverd. Tela (Leningrad)* **32**, 1577 (1990) [*Sov. Phys. Solid State* **32**, 923 (1990)].
- ¹⁶M. I. Kurkin, *Fiz. Tverd. Tela (Leningrad)* **33**, 1805 (1991) [*Sov. Phys. Solid State* **33**, 1014 (1991)].
- ¹⁷V. A. Tulin, *Zh. Éksp. Teor. Fiz.* **55**, 831 (1968) [*Sov. Phys. JETP* **28**, 431 (1968)]; *Zh. Éksp. Teor. Fiz.* **78**, 149 (1980) [*Sov. Phys. JETP* **51**, 73 (1980)].
- ¹⁸A. S. Borovik-Romanov, Yu. M. Bun'kov, B. S. Dumesh *et al.*, *Usp. Fiz. Nauk* **142**, 537 (1984) [*Sov. Phys. Usp.* **27**, 235 (1984)].
- ¹⁹A. G. Gurevich and G. A. Melkov, *Magnetic Oscillations and Waves* [in Russian], Nauka, Moscow (1994), p. 285.
- ²⁰P. M. Richards and L. M. Hinderks, *Phys. Rev.* **183**, 575 (1969).
- ²¹V. T. Adams, L. W. Hinderks, and P. M. Richards, *J. Appl. Phys.* **41**, 931 (1970).
- ²²V. I. Ozhogin and A. Yu. Yakubovsky, *Phys. Lett.* **43**, 505 (1973).
- ²³F. Bloch, *Phys. Rev.* **40**, 460 (1946).
- ²⁴A. F. Andreev and V. I. Marchenko, *Usp. Fiz. Nauk* **130**, 39 (1980) [*Sov. Phys. Usp.* **23**, 21 (1980)].

Translated by James S. Wood